Bioelectrochemistry 139 (2021) 107741

Contents lists available at ScienceDirect

Bioelectrochemistry

journal homepage: www.elsevier.com/locate/bioelechem

Highly sensitive determination of doxorubicin hydrochloride antitumor agent via a carbon nanotube/gold nanoparticle based nanocomposite biosensor

Javid Sharifi [a], Haniyeh Fayazfar [b,*]

[a] Department of Chemical Engineering, Payame Noor University, PO Box 19395-3697, Tehran, Iran
[b] Department of Mechanical and Manufacturing Engineering, Ontario Tech University, Oshawa, ON L1G 0C5, Canada

ARTICLE INFO

Article history:
Received 21 September 2020
Received in revised form 31 December 2020
Accepted 5 January 2021
Available online 12 January 2021

Keywords:
Multi-walled carbon nanotube
Gold nanoparticles
Nanocomposite
Electrochemical sensor
Electrochemical deposition
Doxorubicin hydrochloride

ABSTRACT

A glassy carbon electrode modified with multi-walled carbon nanotubes (MWCNTs) decorated with gold nanoparticles has been investigated for the first time as an ultrasensitive electrochemical sensor for the determination of doxorubicin hydrochloride (DOX), an efficient antitumor agent. The developed nanocomposite has been characterized by scanning electron microscopy (SEM), besides cyclic and linear sweep voltammetry electrochemical techniques. An efficient catalytic activity for the reduction of DOX has been demonstrated, leading to a significant increase in peak current density and a remarkable decrease in reduction over-potential. Under the optimal condition, a wide linear DOX concentration range from 1×10^{-11} to 1×10^{-6} M with a very low detection limit of 6.5 pM was achieved with the modified electrode. Meanwhile, the functionalized MWCNTs/gold nanoparticles indicated an appropriate selectivity, reproducibility, and repeatability as well as long-term stability. The promising outcomes of this research approved the applicability of the developed nanocomposite sensor towards trace amounts of DOX in pharmaceutical and clinical preparations.

1. Introduction

Cancer, a major public health problem and a common primary cause of death around the world, is a term for diseases in which uncontrolled abnormal body cell division happens and can be spread to other parts of the body through the blood and lymph. Treatment alternatives are based on surgical removal, radiotherapy, and chemotherapy where chemotherapy strategies interfere with quite a distinctive cellular and molecular processes having a wide range of anti-neoplastic action and chemotherapeutic applications [1–3]. Doxorubicin hydrochloride (DOX) known by the trade name of "Adriamycin", an efficient antitumor agent, is an antibiotic from the anthracyclines' family which has been extensively used in the treatment of a wide range of cancers. It demonstrates some antitumor activities against a broad spectrum of solid tumors such as breast and lung cancers [3–5]. Although Adriamycin is an efficient antitumor agent, it proved to be highly dose-dependent which shows some severe side effects like local tissue necrosis, myocardial toxicity, cardiotoxicity, liver failure, myelodysplasia, and myelosuppression [5–7]. Therefore, the urgent need for DOX dosage control demands developing effective ways to detect DOX in blood with high sensitivity and low detection limit through a simple, economical, and feasible method.

Scientists have contributed to noteworthy breakthroughs in the determination of pharmaceutical drugs by spectrophotometric, chemiluminescent, high-performance liquid chromatography, photochemical-fluorimetric, microbiological assay method, and electro-analytical techniques with an eye towards sensitivity, rapidity, and simplicity [8–14]. However, compared to most of these techniques which are time-consuming, expensive, and laboring, electrochemical-based methods have been attracted great interest in tackling the analytical challenges and efficient determination of pharmaceutical compounds with numerous advantages such as simplicity, high sensitivity, good selectivity, time and cost-saving [2,15,16].

Meanwhile, positive attention has been also paid to the development of efficient electrochemical sensors to detect DOX and its derivative [17,18]. Various nanomaterials have been used so far to fabricate functional electrodes for DOX detection such as multi-wall carbon nanotubes, Magnetic nanoparticles, Cu nanowires, reduced graphene oxide, poly(2-amino-5-mercapto-1,3,4-thiadiazole), Ag nanoparticles, etc. Although these electrodes are sensitive and selective, they usually suffer from some inevitable

* Corresponding author.
E-mail address: Ramona.fayazfar@ontariotechu.ca (H. Fayazfar).

https://doi.org/10.1016/j.bioelechem.2021.107741
1567-5394/

disadvantages; namely long time analysis, real sample analysis, and complicated sensor fabrication methods [19–25]. To add more, the lowest detection limits achieved so far, have been in the range of 1.5×10^{-4} to 0.77 nm for monoclonal antibody/gold nanoparticles/thiol-based electrode by using electrochemical impedance spectroscopy (EIS) technique, and vertically-ordered mesoporous silica nano-channel film/ reduced graphene oxide by using differential pulse voltammetry (DPV) technique, respectively [19,23]. Therefore, the challenge still remains in the development of an extra-sensitive sensor with a very low detection limit for the trace assay of DOX through a facile and cost-effective approach.

Advanced nanocomposite structures with enhanced properties could be a promising candidate for the development of such highly sensitive modified electrodes. For example, carbon nanotubes in a hybrid configuration with metal nanoparticles can lead to the development of very high electro-active surface areas, promoted electron transfer between electro-active species and electrodes, and synergistic effect [26–29]. Although there are scarce studies investigated the effect of CNTs on electrochemical detection of DOX, not many published researches are available on using CNTs in a composite layout nor on using CNTs and metal nanoparticles in a hybrid configuration to detect DOX by electrochemical techniques. CNT/gold nanostructures hybrid materials have been reported to exhibit high catalytic activity and enhanced electrical conductivity, suggesting broad potential applications in electrochemical sensors and heterogeneous catalysis [26,30,31]. Among various shapes of gold nanostructures, specifically spherical gold nanoparticles, have unique properties such as high redox activity, size- and shape-related optoelectronic properties, large surface-to-volume ratios, excellent biocompatibility, and low toxicity which have attracted much research interest to develop nanocomposite sensors [30–37].

The aforementioned studies encouraged us to develop a highly sensitive nanocomposite electrode based on MWCNTs decorated with gold nanoparticles through a facile template-free and low-cost electrochemical method to detect DOX, for the first time. Also, as an interest and pressing need in using non-toxic electrolytes for gold electro-deposition, we replaced the conventional incompatible cyanide-based bath with non-toxic water-based solution in our work for architectural control of nano-sized gold onto CNTs [26,38–43]. The electrochemical behavior of DOX has been investigated thoroughly at the developed electrodes. A validated sensitive and precise linear sweep voltammetry technique has been used for trace assay of DOX in both bulk form and pharmaceutical formulation. Enhanced synergistic effect of the developed composite nanomaterials led to a very low detection limit, in the picomolar range, high sensitivity, suitable stability, and a large enhancement of linear sweep voltammetry response towards DOX. The outcomes could very well address the essential requirements for a promising long-lasting sensor application in DOX detection.

2. Experimental

2.1. Apparatus and reagents

All electrochemical experiments were carried out by using an Autolab Potentiostat/Galvanostat (PGSTAT 302N, Netherland). We used a conventional three-electrode cell including a working electrode (glassy carbon plate (GCP) substrate with 1.5 cm^2 surface area, modified with MWCNTs/AuNPs), a saturated calomel reference electrode (SCE), and a platinum plate counter electrode. All potential given in this paper were referred to SCE. A MIRA TESCAN field emission scanning electron microscope (FESEM) (operating at 20 kV) was used for morphological characterizations. The Doxorubicin hydrochloride Powder (98.0–102.0% (HPLC)) was obtained from Sigma Aldrich and stored at 4 °C. In addition, the multi-walled carbon nanotubes functionalized with carboxyl groups (20–30 nm diameters, 10–30 μ m length, and >95% purity) were supplied from US Research Nano-materials, Inc. All other chemicals (Merck) had analytical grades with no further purification. Deionized double distilled water (DI-DD water) was used for preparing all solutions. The fresh solution of doxorubicin hydrochloride stock (1×10^{-3} M) was prepared in DI-DD water daily. Different pH values of 0.1 M phosphate buffer solution (PBS) were prepared using Henderson-Hasselback Equation by Na_2HPO_4 and K_2HPO_4 powders and adjusted from 4 to 8 with HCl and $NaOH$ solution. All required DOX solutions were prepared from a stock solution that had been diluted by 0.1 M PBS. A prior de-oxygenation was also carried out by purging high purity nitrogen into the doxorubicin hydrochloride solution at room temperature.

2.2. Synthesis of MWCNTs-COOH/AuNPs/GCP electrode

Prior to the modification of the electrode surface, bare glassy carbon plate was thoroughly polished by 0.05 μm alumina powder and then ultrasonically washed with ethanol, acetone, and DI-DD water for 2 min, respectively, then it was dried at room temperature. Subsequently, 3 mg of MWCNTs were suspended in 10 ml of absolute ethanol in an ultrasonic bath for 30 min. Subsequently, 40 μL of MWCNTs suspension was deposited onto GCP working electrode surface by means of drop-casting method (4 μl each time and let it be dried at room temperature). Thereafter, it was thoroughly washed with DI-DD water to wash away loose powders. The obtained electrode was called MWCNTs-COOH/GCP. Afterward, to synthesize MWCNTs/AuNPs modified electrode, the electrodeposition of AuNPs on MWCNTs was performed by chronoamperometry (the potential-step) technique from an acidic solution of 0.5 M H_2SO_4 containing 5 mM $HAuCl_4$ at +0.2 V applied potential during 10 s. The modified MWCNTs/AuNPs/GCP electrodes were carefully washed with DI-DD water and then dried at room temperature. After that, the modified electrodes (MWCNTs/AuNPs/GCP) were investigated for electrochemical measurements and further analysis. To examine the electro-activity of developed electrodes in DOX reduction, cyclic voltammetry (CV) and linear sweep voltammetry (LSV) techniques have been used. Every measurement was repeated three times with keeping electrodes unchanged. Scheme 1 illustrates the fabrication procedure of the MWCNTs/AuNPs/GCP electrode.

2.3. Optimization method

A stepwise strategy (known as experiments which performed one by one) was applied in order to synthesize the modified electrode and find out optimal parameters which return best possible current response to detect DOX. The following parameters were investigated and optimized; (a) concentration of MWCNTs in absolute ethanol solution; (b) electrodeposition parameters for gold nanoparticles on MWCNTs including solution concentration, time, and potential of deposition; (c) time of pre-concentration for DOX onto the modified electrode prior to each electrochemical measurement; (d) pH values; and (e) scan rate. In short, the following experimental conditions were found to achieve the best results: (a) optimal concentration of MWCNTs; 3 mg MWCNTs in 10 ml of absolute ethanol solution; (b) electro-deposition of AuNPs onto the MWCNTs in 0.5 M H_2SO_4 solution containing 5 mM $HAuCl_4$ at a constant potential of +0.2 V in 10 s; (c) Optimum time for DOX pre-concentration: 120 s; (d) pH value of 7.0; and (e) Scan rate of 100 mVs^{-1}.

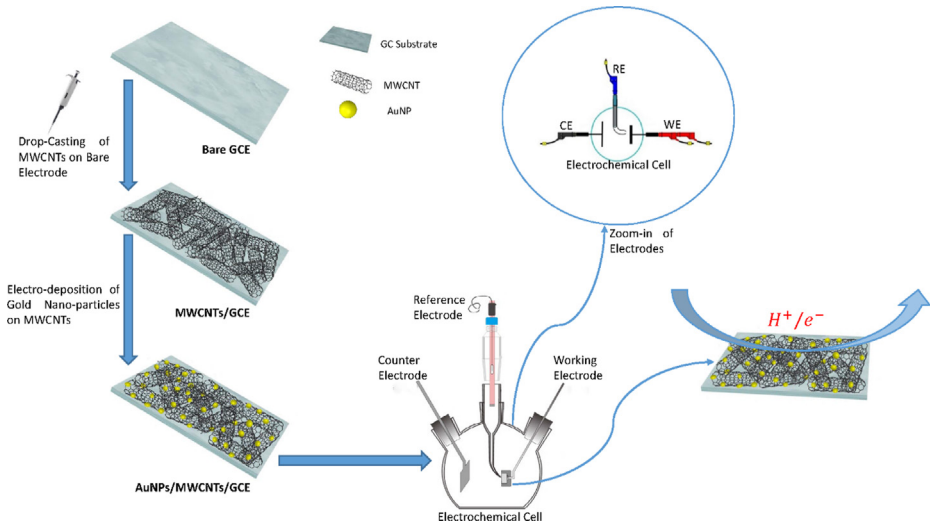

Scheme 1. Schematic representation of the modified electrode (sensor).

3. Results and discussions

3.1. Morphological characterization of the MWCNTs and gold nanoparticles on the glassy carbon plate substrate

Fig. 1a illustrates the drop casted MWCNTs on the well-polished GCP substrate at room temperature characterized by SEM. As it can be seen, the MWCNTs are distributed homogeneously on the substrate, and there are no macro-aggregates on the surface. Also, Fig. 1b shows well-distributed electrodeposited gold nanoparticles (AuNPs) on the MWCNTs. The average diameter of the gold nanoparticles ranged from 20 to 100 nm while in some areas particles grew faster and over-lapped with each other, leading to some aggregates [44].

Fig. 1c represents the chronoamperometry curve for electrodeposition of AuNPs onto the MWCNTs surface in 0.5 M solution H_2SO_4 containing 5 mM $HAuCl_4$ at a constant potential of +0.2 V in 10 s. At the primary stage, the current density increases due to nucleation of gold nanoparticles onto the substrate surface, followed by a growth process which leads to drops in current density as a result of an increase in the concentration gradient of electroactive species on the surface [45,46].

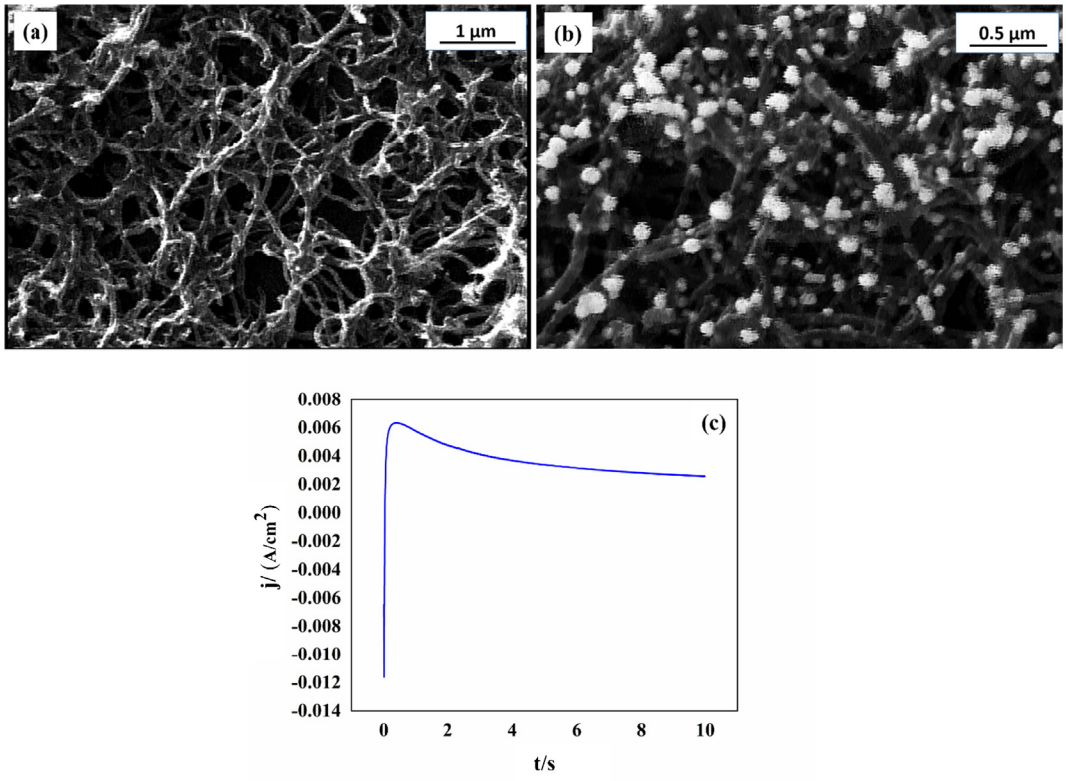

Fig. 1. SEM images showing (a) drop-casted MWCNTs on GCP substrate; (b) Electro-deposited gold nanoparticles on the MWCNTs by the means of chronoamperometry method; (c) chronoamperometry curve for electrodeposition of AuNPs to MWCNTs in 0.5 M solution $\mathbf{H_2SO_4}$ containing 5 mM $\mathbf{HAuCl_4}$ at constant potential of +0.2 V in 10 s.

3.2. Cyclic voltammetry response of different modified electrodes in PBS solution

Fig. 2 illustrates the cyclic voltammetry responses of bare GCP, modified GCP with MWCNTs-COOH, and MWCNTs-COOH/AuNPs/GCP electrodes at the scan rate of 100 mV/s in phosphate buffer solution. Where DOX was not present in the solution, no significant redox peaks were observed for three electrodes. While modification of bare GCP electrode with CNTs (MWCNTs-COOH/GCP electrode) noticeably enhanced the current density, the bare GCP electrode gives a poor current density response. This implies that CNT has significant electro-analytical properties as an active electrode modifier [47]. With further modification of the electrode by Au nanoparticles (MWCNTs-COOH/AuNPs/GCP electrode), the current density enhanced even more compared to the MWCNTs-COOH/GCP. This behavior is due to the electro-catalytic synergistic effect of gold nanoparticles beside carbon nanotubes with enhanced conductivity and high electro-active surface areas [38].

3.3. Cyclic voltammetry response of different electrodes in DOX solution

DOX is an electro-active drug-containing quinone-hydroquinone group which has been studied by numerous researchers and can be identified by the electrochemical reaction of the drug [17,18]. According to previous studies, the redox reactions of these groups are electrochemically reversible and related to Q/QH_2 redox pairs: $Q + 2e^- + 2H^+ \leftrightarrow QH_2$. The reversible two-electron reduction of DOX quinone moiety can be coupled with oxygen reduction by QH_2; thereby, an electron-catalytic cycle can be obtained [17,18].

Fig. 3 compares the cyclic voltammetry responses of different electrodes (both modified and unmodified) in DOX solution (5×10^{-6}M DOX in 0.1 M PBS, pH = 7.0). The CV response of DOX at the bare GCP electrode is shown at Fig. 3a-c. As it can be seen, at the potential range of −0.2 to −0.9 V, a poor redox peak appears, indicating that the bare GCP electrode can slightly respond to DOX detection. At the MWCNTs-COOH/GCP electrode, by contrast, the CV response of DOX was promoted with enlarged current density peaks and negatively shifted peak potential (Fig. 3a–b) due to the fact that MWCNTs-COOH has a large specific surface area and promoted electronic properties. In comparison with MWCNTs-COOH/GCP electrode, the redox of DOX at the MWCNTs-COOH/AuNPs/GCP electrode was significantly increased with the sharper current density peaks. The peak potential also further shifted negatively (Fig. 3a–a). Due to the synergistic effect of the MWCNTs-COOH and gold nanoparticles, this behavior attributes to a strong catalytic function. The MWCNTs-COOH and gold nanoparticles are able to improve the rate of electron transfer due to the high electro-active surface areas, high surface-to-volume ratios, and excellent electrical conductivity [31,33,36]. Hence, in comparison with two other electrodes, the MWCNTS-COOH/AuNPs/GCP modified electrode acts like a super-capacitor to enhance the electrochemical reaction of DOX and promote the rate of electron transfer; consequently, it increases the current density response to the redox of DOX.

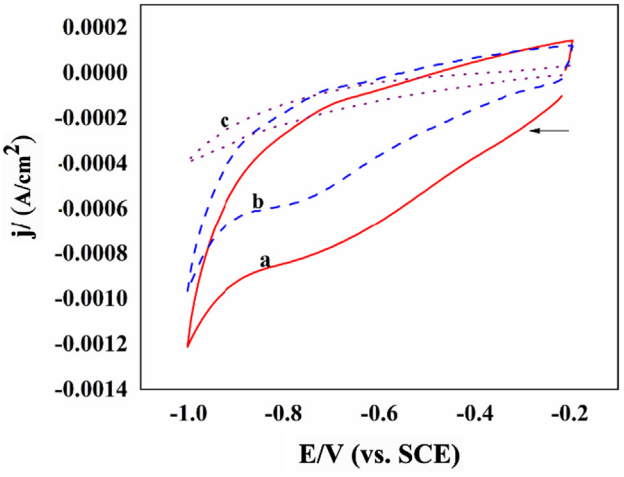

Fig. 2. Cyclic voltammetry responses of 0.1 M PBS (pH = 7.0) at different modified electrodes (a; MWCNTs-COOH/AuNPs/GCP, b; MWCNTs-COOH/GCP, and c; bare GCP electrode); Scan rate 100 mVs-1. (The arrow shows the direction of applying current which started at the potential of −0.2 V).

Fig. 3b shows the sequential cyclic voltammetry responses (3 cycles) for DOX in 0.1 M PBS at MWCNTs-COOH/AuNPs/GCP electrode. The results reveal that the redox reactions of DOX at the modified electrode are completely reversible. The first sweep yields the greatest current density peak height compared to second and third sweeps due to the fact that the redox peak is not only because of the molecules reaching the electrode by diffusion, but also is from those molecules already adsorbed on the electrode surface before the sweep; in subsequent sweeps, the adsorption equilibrium is not achieved, so the diffused molecules cause the signal. At adequately low concentration and high rates of sweep, only the first sweep yields a signal because the number of diffused molecules is insignificant compared to the number of adsorbed molecules [38,48].

Moreover, pH dependency of peak current density and peak potential were investigated over the pH range of 4.0–8.0 via LSV technique in order to determine the most suitable pH for supporting electrolyte (the figure was not shown here). The peak potential negatively shifted with an increase in the pH value; this indicates proton contribution in the electrochemical process [49]. In addition, the peak current density increased with a rise of pH value in the range of 4.0–7.0 and decreased when the pH exceeded 7.0. Therefore, in all voltammetry determinations, PBS with pH 7.0 was used as the supporting electrolyte.

3.4. The effect of scan rates on the DOX electrochemical reaction

Fig. 4a illustrates the effect of potential sweep rates on the DOX reduction reactions at the MWCTNs-COOH/AuNPs/GCP electrode at 5×10^{-6}M DOX, by using a LSV method at different scan rates in the range of 10–200 mV/s. With a slope of 1.0094, the linear relationship between the log ($j_{p,c}$) and the log (υ) (Fig. 4b) confirmed a mix relationship of adsorption and diffusion-controlled processes on the surface of the modified electrode, caused by the adsorption of the DOX species on the electrode surface and their diffusion through the porous MWCNTs-COOH/AuNPs film [38,50]. The following regression equation indicates this relationship:

$$\text{Log}\ (j_{p,c}) = 1.0094\ \text{Log}\ (\upsilon) - 5.7841\ (R^2 = 0.9885,\ j_{p,c}: \text{Acm}^{-2},\ \upsilon: \text{mVs}^{-1})$$

3.5. Linear response of the MWCNTs-COOH/AuNPs/GCP electrode towards DOX and calibration curve

Fig. 5a indicates the applicability study of MWCNTs-COOH/AuNPs/GCP modified electrode in the detection of successive addition of DOX under the optimum conditions (0.1 M PBS (pH = 7) and scan rate of 100 mVs^{-1}) by the LSV technique. The relationship between the various concentrations of DOX and reduction peak current densities were investigated by LSV method on the surface of MWCNTs-COOH/AuNPs/GCP electrode, as shown in Fig. 5b. According to the results, the cathodic peak current density

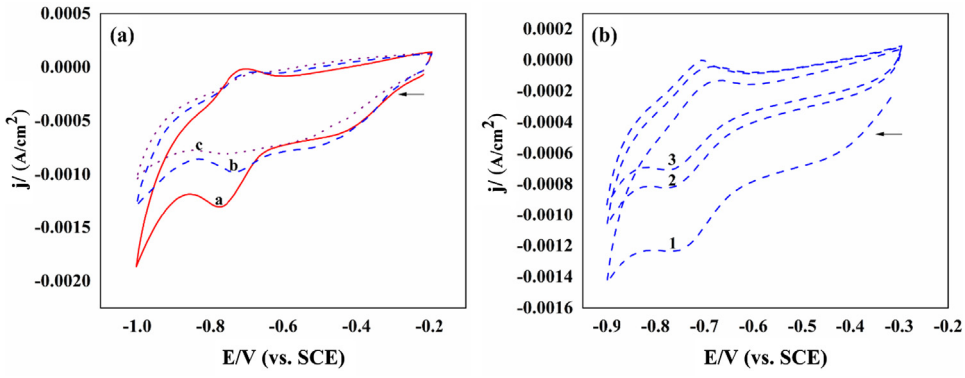

Fig. 3. (a) cyclic voltammetric responses of 5×10^{-6}M DOX in PBS 0.1 M (pH = 7) at the a; MWCNTs-COOH/AuNPs/GCP electrode, b; MWCNTs-COOH/GCP electrode, and c; bare GCP electrode; (b) sequential cyclic voltammetric responses (3 cycles) of 5×10^{-6}M DOX in PBS 0.1 M (pH = 7.0) at MWCNT-COOH/AuNPs/GCP electrode with scan rate of 100 mVs^{-1}, at the potential range from −0.2 to −0.9 V.

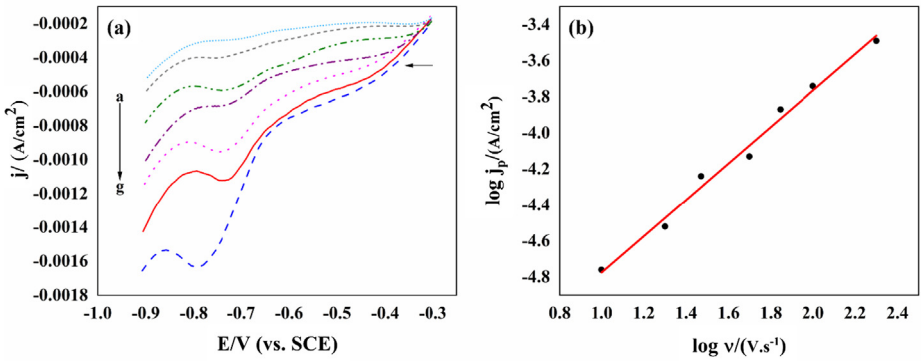

Fig. 4. (a) Linear Sweep Voltammetry responses of the 5×10^{-6} M DOX at the MWCNTs-COOH/AuNPs/GCP electrode at different scan rates (a → g: 10, 20, 30, 50, 70, 100, and 200 mV) in 0.1 M PBS solution (pH = 7.0); (b) the plot of log ($j_{p,c}$) vs. log (υ).

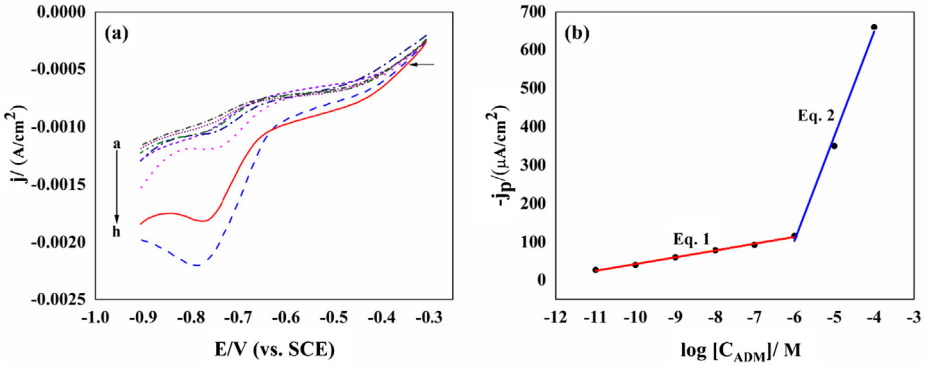

Fig. 5. (a) the LSV response of DOX with various concentrations in the range of $1 \times 10^{-11} - 1 \times 10^{-4}$M in 0.1 M PBS solution (a → h:$1 \times (10^{-11} \rightarrow 10^{-4})$ M; pH = 7). (b), corresponding linear calibration curve of peak current vs. DOX concentration. Scan rate of 100 mVs^{-1}; Eq.1 refers to $j_{p,c}$ = 2018.78 + 17.543 log [C]/M (R^2 = 0.9953) and Eq.2 refers to $j_{p,c}$ = 1735.3 + 272 log [C]/M (R^2 = 0.9935).

increased with an increase in the DOX concentration. The conventional calibration curve by plotting peak current density versus the concentration demonstrated a non-linear curve. For this reason, and because of rather a wide range of concentration determined, empirical semi-logarithmic model (peak current density vs. logarithm of concentration) is recommended during data analysis to view the data easily and to facilitate evaluation of the assay performance [51–53]. The variation of the peak current densities was linearly proportional to logarithm of DOX concentration in two intervals in the concentration range of $1 \times 10^{-6} - 1 \times 10^{-11}$ M, and $1 \times 10^{-4} - 1 \times 10^{-6}$M in 0.1 M phosphate buffer solution (pH = 7.0), illustrating a wide range of DOX detection by the modified electrode, and in this particular case, shows that DOX acts in a concentration-dependent manner [54].The linear regression equations between the reduction signals of the sensor and the logarithm of the DOX concentration are as bellows:

$$j_{p,c}(\mu A\ cm^{-2}) = 218.78 + 17.543\ Log\ [C]/M, \quad \left(R^2 = 0.9953\right) \qquad (1)$$

for $1 \times 10^{-6} - 1 \times 10^{-11}$ M DOX, and

$$j_{p,c}(\mu A\ cm^{-2}) = 1735.3 + 272\ Log\ [C]/M,\ R^2 = (0.9935) \quad (2)$$

for $1 \times 10^{-4} - 1 \times 10^{-6}$M DOX

At high concentrations, an increase of the slope has been observed which could be due to the adsorption-diffusion mixed controlled process (adsorption and diffusion of DOX's reduction products on the electrode surface), while at sufficiently low concentrations, only adsorption mechanism caused the signal [38]. Hence, a change in the slope could be resulted due to the conversion of controlled-process and kinetic limitations [22,34,38].

The detection limit of DOX was estimated to be 6.5×10^{-3}nM (with signal-to-noise of 3) using the first range of the calibration plot ($1 \times 10^{-6} - 1 \times 10^{-11}$ M DOX). In comparison with the previously reported studies, as shown in Table 1, the proposed electrode is the first one of its kind which uses multi-wall carbon nanotubes in a nanocomposite configuration with gold nanoparticles, leading to extra sensitive bio-nanosensor with a very low detection limit in DOX determination. It is worth mentioning that the electrochemical sensor based on a specific monoclonal antibody-gold nanoparticle reported by B. Rezaei group [19], as a sensitive DOX impedimetric immunosensor with the detection limit of 1.5×10^{-4} nM, suffers from complicated and time-consuming fabrication process. Furthermore, the electrode operates at acidic pH required for redox activity which limits the application of this biosensor in biological fluids. In our work, a facile and affordable electrochemical method has been developed in phosphate buffer solution with the pH of 7, addressing some of the major drawbacks of the current state-of-the-art.

3.6. Reproducibility, repeatability and stability of the MWCNTs-COOH/AuNPs/GCP modified electrode

Three following parameters must be considered to evaluate the performance of an effective sensor: the stability, reproducibility, and repeatability of the response. In order to investigate the reproducibility of the proposed electrode, a relative standard deviation (RSD) of 3.4% was obtained for the averages of six determinations on every single modified electrode independently under the same fabrication procedure at 5×10^{-6} M DOX. The stability of the modified sensor was also examined; MWCNTs-COOH/AuNPs/GCP electrode was stored under the circumfused condition over an interval of 2 weeks, the electrode kept 94.7% of its initial peak current density response for a DOX concentration of 5×10^{-6} M which showed long-term stability of the modified electrode. The same electrode was repeatedly examined in 5×10^{-6} M DOX in 0.1 M PBS (pH = 7.0) in order to inspect the repeatability of the modified electrode. An insignificant change in the peak current density was observed. Therefore, the results showed that the modified electrode has an appropriate reproducibility and repeatability with long-term stability in both preparation procedure and voltammetry determinations.

3.7. The selectivity of the MWCNTs-COOH/AuNPs/GCP modified electrode over the coexisting chemical interferences

To assess the selectivity of the proposed sensor, LSV technique was used to check the interference of ascorbic acid (AA), uric acid (UA), L-cystine, glucose, and tyrosine in DOX solution (5×10^{-6}M DOX in 0.1 M PBS, pH = 7.0) at the potential range of −0.3 to −0.9 V. Each of the aforementioned materials was examined separately in 0.1 M PBS containing DOX at the potential range of −0.3 to −0.9 V and no obvious interference peaks were observed in this range. Therefore, these materials did not show any interferences in DOX detection with no significant effect on the electrochemical responses of the proposed electrode. As a result, the modified MWCNTs-COOH/AuNPs/GCP electrode demonstrated a very good selectivity in DOX reduction. The voltammetry behavior of ascorbic acid, uric acid, L-cystine, glucose, and tyrosin reported in previous studies also confirmed that these materials represent no reduction peaks for DOX in the range of investigated potential in this work [55,57–64].

3.8. Analytical application in real samples

The LSV procedure was effectively applied to the MWCTNs/AuNPs/GCP electrode in DOX injection to determine DOX in pharmaceutical dosage form of DOX injection as well as asses the applicability of the proposed method towards clinical determinations. Furthermore, both calibration curve and the standard addition method were used to assess the validity (Table 2). No further efforts were made for assays of DOX in real samples but dilution to obtain 5×10^{-6} M DOX. The obtained results demonstrated that the sterile powder of DOX injection real sample has shown no intervention on the electrochemical investigation of DOX. Moreover, in order to calculate the accuracy on the recovery of precise volume of the standard DOX injection, real solution spiked in bulk DOX solution at five levels. According to the demonstrated outcomes in Table 2, recoveries were in the range of 95.27–104.2%, which indicating satisfactory accuracy and precision for the developed method, suggesting the successful applicability of the proposed process for the scientific and clinical applications as well.

Table 1
A review on electrochemical studies of doxorubicin hydrochloride.

Methods		Materials	Linear Range (M) ($\times 10^{-9}$)	LoD (nM)	pH	Ref
Electrochemistry	**LSV**	**MWCNTs/AuNPs/GCP**	**0.01–1000**	6.5×10^{-3}	**7**	**This Work**
	EIS	MAb[a]/GNP[b]/TBSol-Gel[c]/GE[d]	0.00017–0.43	1.5×10^{-4}	5	[19]
	DPV	PAMT[e]/AuNPs/rGO[f]/GCE	0.003–30,000	9×10^{-3}	7	[20]
	CV	Poly(Azure B-Proflavine)/GCE	0.03–10	0.01	7	[21]
	CV	Poly (Azure B)/GCE	100–0.3	0.1	5	[22]
	DPV	VMSF[g]/ErGo[h]	1–20,000	0.77	6	[23]
Fluorometry		L-Trp/AuAgNCs[i]	2500–150,000	3	3	[24]

[a] Monoclonal antibody.
[b] Gold nanoparticles.
[c] Thiol-based sol–gel.
[d] Gold Electrode.
[e] Poly(2-amino-5-mercapto-1,3,4-thiadiazole).
[f] Reduced graphene oxide.
[g] Vertically-ordered mesoporous silica nano-channel film.
[h] Electrochemically reduced graphene oxide.
[i] Gold/silver nanoclusters.

Table 2
Results of the recovery analysis of DOX spiked in real samples.

No	Spiked (μM)	Expected (μM)	Found[a] (μM)	Recovery (%)
1	0	5	4.91	–
2	0.5	5.5	5.24	95.27
3	1	6	6.21	103.5
4	5	10	10.3	103
5	10	15	15.63	104.2
6	50	60	59.76	99.6

4. Conclusion

As an advanced nanocomposite material, a MWCNTs-COOH/AuNPs modified electrode based on electrochemical growth of gold nanoparticles on MWCNTs-COOH surface was introduced to investigate the electrochemical behavior of doxorubicin hydrochloride, for the first time. The proposed LSV technique provided significant advantages such as rapidity, simplicity, and preciseness, successfully employed for DOX trace in bulk form and pharmaceutical formulation. The developed nanocomposite sensor indicated enhanced electro-catalytic activity, high stability and repeatability, and satisfactory selectivity for DOX detection. The wisely combination of MWCNTs and gold nanoparticles led to a synergistic effect to improve the rate of electron transfer and prepare an active platform for highly sensitive determination of DOX. A broad range of DOX concentration from 1×10^{-11} to 1×10^{-4} M with the detection limit of 6.5×10^{-3} nM (signal-to-noise of 3) was detected under optimized condition, showing high sensitivity of the modified electrode. To the best of our knowledge, it is the lowest amount of detection limit among the most significant reported results so far [19–24]. The promising outcomes of the proposed research could be very well become a satisfying candidate for the determination of the trace amounts of DOX in pharmaceutical and clinical preparations in the near future.

Declaration of Competing Interest

The authors declare that they have no known competing financial interests or personal relationships that could have appeared to influence the work reported in this paper.

References

[1] R. Hajian, Z. Tayebi, N. Shams, Fabrication of an electrochemical sensor for determination of doxorubicin in human plasma and its interaction with DNA, J. Pharm. Anal. 7 (2017) 27–33, https://doi.org/10.1016/j.jpha.2016.07.005.

[2] D. Hynek, L. Krejcova, O. Zitka, V. Adam, L. Trnkova, J. Sochor, M. Stiborova, T. Eckschlager, J. Hubalek, R. Kizek, Electrochemical study of doxorubicin interaction with different sequences of double stranded oligonucleotides, Part II, Int. J. Electrochem. Sci. 7 (2012) 34–49.

[3] K. Zhang, Y. Zhang, Electrochemical behavior of adriamycin at an electrode modified with silver nanoparticles and multi-walled carbon nanotubes, and its application, Microchim. Acta 169 (2010) 161–165, https://doi.org/10.1007/s00604-010-0331-3.

[4] O.O. Krasnovskaya, V.M. Malinnikov, N.S. Dashkova, V.M. Gerasimov, I.V. Grishina, I.I. Kireev, S.V. Lavrushkina, P.A. Panchenko, M.A. Zakharko, P.A. Ignatov, O.A. Fedorova, G. Jonusauskas, D.A. Skvortsov, S.S. Kovalev, E.K. Beloglazkina, N.V. Zyk, A.G. Majouga, Thiourea modified doxorubicin: a perspective pH-sensitive prodrug, Bioconjug. Chem. 30 (2019) 741–750, https://doi.org/10.1021/acs.bioconjchem.8b00885.

[5] S. Zhang, X. Liu, T. Bawa-Khalfe, L.S. Lu, Y.L. Lyu, L.F. Liu, E.T.H. Yeh, Identification of the molecular basis of doxorubicin-induced cardiotoxicity, Nat. Med. 18 (2012) 1639–1642, https://doi.org/10.1038/nm.2919.

[6] Y. Octavia, C.G. Tocchetti, K.L. Gabrielson, S. Janssens, H.J. Crijns, A.L. Moens, Doxorubicin-induced cardiomyopathy: from molecular mechanisms to therapeutic strategies, J. Mol. Cell. Cardiol. 52 (2012) 1213–1225, https://doi.org/10.1016/j.yjmcc.2012.03.006.

[7] C.S. Abdullah, S. Alam, R. Aishwarya, S. Miriyala, M.A.N. Bhuiyan, M. Panchatcharam, C.B. Pattillo, A.W. Orr, J. Sadoshima, J.A. Hill, M.S. Bhuiyan, Doxorubicin-induced cardiomyopathy associated with inhibition of autophagic degradation process and defects in mitochondrial respiration, Sci. Rep. 9 (2019) 1–20, https://doi.org/10.1038/s41598-018-37862-3.

[8] E.A. Dil, M. Ghaedi, A. Asfaram, Application of hydrophobic deep eutectic solvent as the carrier for ferrofluid: a novel strategy for pre-concentration and determination of mefenamic acid in human urine samples by high performance liquid chromatography under experimental design optimizat, Talanta 202 (2019) 526–530, https://doi.org/10.1016/j.talanta.2019.05.027.

[9] Y.B. Monakhova, U. Holzgrabe, B.W.K. Diehl, Current role and future perspectives of multivariate (chemometric) methods in NMR spectroscopic analysis of pharmaceutical products, J. Pharm. Biomed. Anal. 147 (2018) 580–589, https://doi.org/10.1016/j.jpba.2017.05.034.

[10] A. Alevridis, A. Tsiasioti, C.K. Zacharis, P.D. Tzanavaras, Fluorimetric method for the determination of histidine in random human urine based on zone fluidics, Molecules 25 (2020), https://doi.org/10.3390/molecules25071665.

[11] B. Zanfrognini, L. Pigani, C. Zanardi, Recent advances in the direct electrochemical detection of drugs of abuse, J. Solid State Electrochem. 24 (2020) 2603–2616, https://doi.org/10.1007/s10008-020-04686-z.

[12] S. Rauf, J.J. Gooding, K. Akhtar, M.A. Ghauri, M. Rahman, M.A. Anwar, A.M. Khalid, Electrochemical approach of anticancer drugs-DNA interaction, J. Pharm. Biomed. Anal. 37 (2005) 205–217, https://doi.org/10.1016/j.jpba.2004.10.037.

[13] J. Fu, X. An, Y. Yao, Y. Guo, X. Sun, Electrochemical aptasensor based on one step co-electrodeposition of aptamer and GO-CuNPs nanocomposite for organophosphorus pesticide detection, Sensors Actuators, B Chem. 287 (2019) 503–509, https://doi.org/10.1016/j.snb.2019.02.057.

[14] X. Shi, J. Sun, Y. Yao, H. Liu, J. Huang, Y. Guo, X. Sun, Novel electrochemical aptasensor with dual signal amplification strategy for detection of acetamiprid, Sci. Total Environ. 705 (2020), https://doi.org/10.1016/j.scitotenv.2019.135905.

[15] N. Dubey, C.S. Kushwaha, S.K. Shukla, A review on electrically conducting polymer bionanocomposites for biomedical and other applications, Int. J. Polym. Mater. Polym. Biomater. 69 (2020) 709–727, https://doi.org/10.1080/00914037.2019.1605513.

[16] N.A. Mungroo, S. Neethirajan, Biosensors for the detection of antibiotics in poultry industry – a review, Biosensors 4 (2014) 472–493, https://doi.org/10.3390/bios4040472.

[17] E.M. Materon, A. Wong, O. Fatibello-Filho, R.C. Faria, Development of a simple electrochemical sensor for the simultaneous detection of anticancer drugs, J. Electroanal. Chem. 827 (2018) 64–72, https://doi.org/10.1016/j.jelechem.2018.09.010.

[18] A. Khanmohammadi, A. Aghaie, E. Vahedi, A. Qazvini, M. Ghanei, A. Afkhami, A. Hajian, H. Bagheri, Electrochemical biosensors for the detection of lung cancer biomarkers: a review, Talanta 206 (2020), https://doi.org/10.1016/j.talanta.2019.120251.

[19] B. Rezaei, N. Askarpour, A.A. Ensafi, A novel sensitive doxorubicin impedimetric immunosensor based on a specific monoclonal antibody-gold nanoaprticle-sol-gel modified electrode, Talanta 119 (2014) 164–169, https://doi.org/10.1016/j.talanta.2013.11.017.

[20] M.H. Ghanbari, F. Shahdost-Fard, H. Salehzadeh, M.R. Ganjali, M. Iman, M. Rahimi-Nasrabadi, F. Ahmadi, A nanocomposite prepared from reduced graphene oxide, gold nanoparticles and poly(2-amino-5-mercapto-1,3,4-thiadiazole) for use in an electrochemical sensor for doxorubicin, Microchim. Acta 186 (2019), https://doi.org/10.1007/s00604-019-3761-6.

[21] A. Porfireva, G. Evtugyn, Electrochemical DNA sensor based on the copolymer of proflavine and Azure B for doxorubicin determination, Nanomaterials. 10 (2020) 1–16, https://doi.org/10.3390/nano10050924.

[22] A. Porfireva, V. Vorobev, S. Babkina, G. Evtugyn, Electrochemical sensor based on Poly(Azure B)-DNA composite for doxorubicin determination, Sensors (Switzerland) 19 (2019) 1–14, https://doi.org/10.3390/s19092085.

[23] F. Yan, J. Chen, Q. Jin, H. Zhou, A. Sailjoi, J. Liu, W. Tang, Fast one-step fabrication of a vertically-ordered mesoporous silica-nanochannel film on graphene for direct and sensitive detection of doxorubicin in human whole blood, J. Mater. Chem. C 8 (2020) 7113–7119, https://doi.org/10.1039/d0tc00744g.

[24] F. Meng, F. Gan, G. Ye, Bimetallic gold/silver nanoclusters as a fluorescent probe for detection of methotrexate and doxorubicin in serum, Microchim. Acta 186 (2019), https://doi.org/10.1007/s00604-019-3477-7.

[25] A.A. Saeed, J.L.A. Sánchez, C.K. O'Sullivan, M.N. Abbas, DNA biosensors based on gold nanoparticles-modified graphene oxide for the detection of breast cancer biomarkers for early diagnosis, Bioelectrochemistry 118 (2017) 91–99, https://doi.org/10.1016/j.bioelechem.2017.07.002.

[26] B. Wu, Y. Kuang, X. Zhang, J. Chen, Noble metal nanoparticles/carbon nanotubes nanohybrids: synthesis and applications, Nano Today 6 (2011) 75–90, https://doi.org/10.1016/j.nantod.2010.12.008.

[27] J.-M. Yeh, K.-Y. Huang, S.-Y. Lin, Y.-Y. Wu, C.-C. Huang, S.-J. Liou, Noncovalent interaction between gold nanoparticles and multiwalled carbon nanotubes via an intermediatory, J. Nanotechnol. 2009 (2009) 1–7, https://doi.org/10.1155/2009/217469.
[28] H. Yang, W. Xu, X. Liang, Y. Yang, Y. Zhou, Carbon nanotubes in electrochemical, colorimetric, and fluorimetric immunosensors and immunoassays: a review, Microchim. Acta 187 (2020) 1–18, https://doi.org/10.1007/s00604-020-4172-4.
[29] G.A. Rivas, M.D. Rubianes, M.C. Rodríguez, N.F. Ferreyra, G.L. Luque, M.L. Pedano, S.A. Miscoria, C. Parrado, Carbon nanotubes for electrochemical biosensing, Talanta 74 (2007) 291–307, https://doi.org/10.1016/j.talanta.2007.10.013.
[30] A. Muhammad, N.A. Yusof, R. Hajian, J. Abdullah, Construction of an electrochemical sensor based on carbon nanotubes/gold nanoparticles for trace determination of amoxicillin in bovine milk, Sensors (Switzerland) 16 (2016) 1–13, https://doi.org/10.3390/s16010056.
[31] N. Ben Messaoud, M.E. Ghica, C. Dridi, M. Ben Ali, C.M.A. Brett, Electrochemical sensor based on multiwalled carbon nanotube and gold nanoparticle modified electrode for the sensitive detection of bisphenol A, Sens. Actuators B Chem. 253 (2017) 513–522, https://doi.org/10.1016/j.snb.2017.06.160.
[32] R. Hajian, N.A. Yusof, T. Faragi, N. Shams, Fabrication of an electrochemical sensor based on gold nanoparticles/carbon nanotubes as nanocomposite materials: determination of myricetin in some drinks, PLoS ONE 9 (2014) 1–7, https://doi.org/10.1371/journal.pone.0096686.
[33] M. Masikini, M.E. Ghica, P.G.L. Baker, E.I. Iwuoha, C.M.A. Brett, Electrochemical sensor based on multi-walled carbon nanotube/gold nanoparticle modified glassy carbon electrode for detection of estradiol in environmental samples, Electroanalysis 31 (2019) 1925–1933, https://doi.org/10.1002/elan.201900190.
[34] W. Da Silva, M.E. Ghica, C.M.A. Brett, Gold nanoparticle decorated multiwalled carbon nanotube modified electrodes for the electrochemical determination of theophylline, Anal. Methods 10 (2018) 5634–5642, https://doi.org/10.1039/c8ay02150c.
[35] A. Muhammad, R. Hajian, N.A. Yusof, N. Shams, J. Abdullah, P.M. Woi, H. Garmestani, A screen printed carbon electrode modified with carbon nanotubes and gold nanoparticles as a sensitive electrochemical sensor for determination of thiamphenicol residue in milk, RSC Adv. 8 (2018) 2714–2722, https://doi.org/10.1039/c7ra07544h.
[36] M. Das, K.H. Shim, S.S.A. An, D.K. Yi, Review on gold nanoparticles and their applications, Toxicol. Environ. Health Sci. 3 (2011) 193–205, https://doi.org/10.1007/s13530-011-0109-y.
[37] Y.C. Yeh, B. Creran, V.M. Rotello, Gold nanoparticles: Preparation, properties, and applications in bionanotechnology, Nanoscale. 4 (2012) 1871–1880, https://doi.org/10.1039/c1nr11188d.
[38] H. Fayazfar, A. Afshar, A. Dolati, Tantalum electrodes modified with well-aligned carbon nanotube-au nanoparticles: application to the highly sensitive electrochemical determination of cefazolin, Appl. Biochem. Biotechnol. 173 (2014) 1511–1528, https://doi.org/10.1007/s12010-014-0944-9.
[39] A.J. Saleh Ahammad, J.J. Lee, M.A. Rahman, Electrochemical sensors based on carbon nanotubes, Sensors. 9 (2009) 2289–2319, https://doi.org/10.3390/s90402289.
[40] C. Ferrag, K. Kerman, Grand challenges in nanomaterial-based electrochemical sensors, Front. Sens. 1 (2020), https://doi.org/10.3389/fsens.2020.583822.
[41] A. Chen, S. Chatterjee, Nanomaterials based electrochemical sensors for biomedical applications, Chem. Soc. Rev. 42 (2013) 5425–5438, https://doi.org/10.1039/c3cs35518g.
[42] N. Moghimian, M. Sam, J.D. Coelho, S.D.W. Warwick, R.B. Bhiladvala, Suppressing electroless growth allows cyanide-free electrodeposition of straight separable gold nanowires, Electrochim. Acta 114 (2013) 643–648, https://doi.org/10.1016/j.electacta.2013.10.107.
[43] I. Khan, K. Saeed, I. Khan, Nanoparticles: properties, applications and toxicities, Arab. J. Chem. 12 (2019) 908–931, https://doi.org/10.1016/j.arabjc.2017.05.011.
[44] H. Fayazfar, A. Afshar, M. Dolati, A. Dolati, DNA impedance biosensor for detection of cancer, TP53 gene mutation, based on gold nanoparticles/aligned carbon nanotubes modified electrode, Anal. Chim. Acta 836 (2014) 34–44, https://doi.org/10.1016/j.aca.2014.05.029.
[45] H. Fayazfar, A. Afshar, A. Dolati, Electrodeposition of various Au nanostructures on aligned carbon nanotubes as highly sensitive nanoelectrode ensembles, J. Mater. Eng. Perform. 24 (2015) 2005–2015, https://doi.org/10.1007/s11665-015-1453-x.
[46] A. Dolati, M. Ghorbani, M.R. Ahmadi, An electrochemical study of Au-Ni alloy electrodeposition from cyanide-citrate electrolytes, J. Electroanal. Chem. 577 (2005) 1–8, https://doi.org/10.1016/j.jelechem.2004.10.024.
[47] C.B. Jacobs, M.J. Peairs, B.J. Venton, Review: carbon nanotube based electrochemical sensors for biomolecules, Anal. Chim. Acta 662 (2010) 105–127, https://doi.org/10.1016/j.aca.2010.01.009.
[48] Z. Gong, G. Zhang, S. Wang, Electrochemical reduction of oxygen on anthraquinone/carbon nanotubes nanohybrid modified glassy carbon electrode in neutral medium, J. Chem. 2013 (2013) 20–27, https://doi.org/10.1155/2013/756307.
[49] M. Revenga-Parra, F. Pariente, E. Lorenzo, Chemically Modified Graphene-based Screen-printed Electrodes for Electrocatalytic Applications, Elsevier, 2018, https://doi.org/10.1016/B978-0-12-409547-2.13373-6.
[50] R.S. Nicholson, I. Shain, Stationary electrode polarography, Anal. Chem. 36 (1964) 706–723.
[51] E. Desimoni, B. Brunetti, Environmental Analysis by Electrochemical Sensors and Biosensors, Environ. Anal. Electrochem. Sens. Biosens. (2015) 1137–1151, https://doi.org/10.1007/978-1-4939-1301-5_18.
[52] M. Azadeh, B. Gorovits, J. Kamerud, S. MacMannis, A. Safavi, J. Sailstad, P. Sondag, Calibration curves in quantitative ligand binding assays: recommendations and best practices for preparation, design, and editing of calibration curves, AAPS J. 20 (2018), https://doi.org/10.1208/s12248-017-0159-4.
[53] D.R. Thvenot, K. Toth, R.A. Durst, G.S. Wilson, Electrochemical biosensors: recommended definitions and classification (Technical Report), Pure Appl. Chem. 71 (1999) 2333–2348, https://doi.org/10.1351/pac199971122333.
[54] H. Ilkhani, T. Hughes, J. Li, C.J. Zhong, M. Hepel, Nanostructured SERS-electrochemical biosensors for testing of anticancer drug interactions with DNA, Biosens. Bioelectron. 80 (2016) 257–264, https://doi.org/10.1016/j.bios.2016.01.068.
[55] Y. Li, W. Ye, Y. Cui, B. Li, Y. Yang, G. Qian, A metal-organic frameworks@ carbon nanotubes based electrochemical sensor for highly sensitive and selective determination of ascorbic acid, J. Mol. Struct. 1209 (2020), https://doi.org/10.1016/j.molstruc.2020.127986.
[57] M. Rees, A.G. Wright, S. Holdcroft, P. Bertoncello, Voltammetry at hexamethyl-p-terphenyl poly(Benzimidazolium) (HMT-PMBI)-coated glassy carbon electrodes: charge transport properties and detection of uric and ascorbic acid, Sensors (Switzerland) 20 (2020), https://doi.org/10.3390/s20020443.
[58] X. Pang, F. Li, S. Huang, Z. Yang, Q. Mo, L. Huang, W. Xu, L. Chen, X. Li, Electrostatically mediated layer-by-layer assembly of nitrogen-doped graphene/PDDA/gold nanoparticle composites for electrochemical detection of uric acid, Anal. Bioanal. Chem. 412 (2020) 669–680, https://doi.org/10.1007/s00216-019-02275-2.
[59] M.I. Shekh, J. Amirian, B. Du, A. Kumar, G. Sharma, F.J. Stadler, J. Song, Electrospun ferric ceria nanofibers blended with MWCNTs for high-performance electrochemical detection of uric acid, Ceram. Int. 46 (2020) 9050–9064, https://doi.org/10.1016/j.ceramint.2019.12.153.
[60] Z. Khosroshahi, F. Karimzadeh, M. Kharaziha, A. Allafchian, A non-enzymatic sensor based on three-dimensional graphene foam decorated with Cu-xCu2O nanoparticles for electrochemical detection of glucose and its application in human serum, Mater. Sci. Eng.: C (2020), https://doi.org/10.1016/j.msec.2019.110216.
[61] R. Ahmad, M. Khan, M.R. Khan, N. Tripathy, M.I.R. Khan, P. Mishra, M.A. Syed, A. Khosla, Nano-donuts shaped nickel oxide nanostructures for sensitive non-enzymatic electrochemical detection of glucose, Microsyst. Technol. 4 (2020), https://doi.org/10.1007/s00542-020-04754-4.
[62] R. Jerome, P.V. Keerthivasan, N. Murugan, N.R. Devi, A.K. Sundramoorthy, Preparation of stable CuO/boron nitride nanocomposite modified electrode for selective electrochemical detection of L-cysteine, ChemistrySelect. 5 (2020) 9111–9118, https://doi.org/10.1002/slct.202002105.
[63] K. Murtada, R. Salghi, A. Ríos, M. Zougagh, A sensitive electrochemical sensor based on aluminium doped copper selenide nanoparticles-modified screen printed carbon electrode for determination of L-tyrosine in pharmaceutical samples, J. Electroanal. Chem. 874 (2020), https://doi.org/10.1016/j.jelechem.2020.114466.
[64] G. Wang, J. Sun, Y. Yao, X. An, H. Zhang, G. Chu, S. Jiang, Y. Guo, X. Sun, Y. Liu, Detection of inosine monophosphate (IMP) in meat using double-enzyme sensor, Food Anal. Methods 13 (2020) 420–432, https://doi.org/10.1007/s12161-019-01652-y.